ISSN print: 1224-5984
ISSN online: 2248-3942

Rom Biotechnol Lett. 2022; 27(6): 3768-3778
doi: 10.25083/rbl/27.6/3768.3778

Received for publication, March, 13, 2023
Accepted, April, 20, 2023

Original article

MicroRNA 138 upregulation is associated with decreasing levels of CCND1 gene expression and promoting cell death in human prostate cancer cell lines

NASRIN HAGHIGHI-NAJAFABADI[1], SHIMA FAYAZ[2], GHAZAL HADDAD[3], MAHBOUBEH BERIZI[2], PEZHMAN FARD-ESFAHANI[2]*

[1] Molecular Medicine Department, Biotechnology Research Center, Pasteur Institute of Iran, Iran
[2] Biochemistry Department, Pasteur Institute of Iran, Iran
[3] Faculty of Medicine, University of Toronto, Toronto, Ontario, Canada

Abstract

This research intended to discover the significance of miR-138 on the expression profile, proliferation, and the associated regulatory mechanisms in prostate cancer (PCa). RT-qPCR was applied to compare the expression of miR-138 in the PCa cells with a non-cancer cell line, as well as PCa tissue samples with benign prostatic hyperplasia (BPH) samples. The expression of miR-138 notably diminished in PCa tissues and cell lines. Afterward, formerly documented genes, along with bioinformatics analysis, suggested seven possible target genes of miR-138. Among them, *CCND1* seemed to have higher expression in the PCa cell lines and tissues. Also, the negative correlation of miR-138 and *CCND1* in PCa cell line and tissues was validated using Pearson correlation. CCDN1 was revealed to be the target gene of miR138 in the PC3 cell line based on the results of the luciferase reporter gene assay. Over-expression of miR138-5p suppressed the expression of CCDN1 in PCa cell lines as exhibited by RT-qPCR. Finally, the results of the MTT assay exhibited the inhibitory impact of miR-138 on the proliferative capacities in PCa cell lines. Our research introduces miR-138 as a negative regulator of *CCDN1* in the progression of PCa with an inhibitory impact on the proliferation rate of prostate cancer (PCa) cell lines. This regulatory mechanism could be utilized for the design and target selection of remedial miRNA-based approaches.

Keywords miRNA, miR-138, *CCND1*, Prostate cancer, oncogene, tumor suppressor

To cite this article: NASRIN HAGHIGHI-NAJAFABADI. MicroRNA 138 upregulation is associated with decreasing levels of CCND1 gene expression and promoting cell death in human prostate cancer cell lines. *Rom Biotechnol Lett.* 2022; 27(6): 3768-3778 DOI: 10.25083/rbl/27.6/3768.3778

*Corresponding author: Pezhman Fard-Esfahani, Department of Biochemistry, Pasteur Institute of Iran, Tehran, Iran. Tel: +989122171687; Email: fard-esfahani@pasteur.ac.ir; pejman_fard@yahoo.com

Introduction

The second most predominant type of malignant cancer is Prostate cancer (PCa). It is also the fifth primary reason for cancer-related death in men in the world (1). Serum prostate-specific antigen (PSA) measure and digital rectal examination are the most extensively utilized PCa screening instruments. Even though serum PSA facilitated the diagnosis of PCa at initial disease stages but high false-positive sounds as a significant disadvantage (2). Hence, a more specific PCa biomarker would be helpful in improving PCa screening. Other biomarkers, including PCA3 score, Prostate Health Index (PHI), and 4Kscore, were recommended to ameliorate the accuracy of PSA prognosis (3). Moreover, cancer-related microRNAs (miRNAs) appeared as promising candidates in the diagnosis, prognosis, and treatment of cancer (4).

MiRNAs are single-stranded noncoding RNA molecules (18-24 nucleotides) that bind to the 3′-untranslated region (3′-UTR) of target mRNA to repress gene expression post-transcriptionally (5). MiRNA expression signatures are dissimilar between cancer and normal tissue and distinct cancer subtypes (6). More importantly, well-provided evidence has emphasized the anomalous expression of miRNAs in the malignancy of cancers (7, 8). Therefore, miRNAs as cancer-specific biomarkers can be used to alleviate diagnosis, prognosis, and outcome of the therapy (9).

MiR-138 were attended as a tumor suppressor in numerous malignancies, including prostate, pancreatic, nasopharyngeal, colorectal, osteosarcoma, non-small cell lung cancers, and other malignant tumors (10-15). MiR-138 has the tumor suppressor function via diverse mechanisms such as apoptosis motivation, suppression of proliferation, metastasis, invasion, and modification of chemosensitivity in tumor cells. Distinct mechanisms imply heterogeneous targets of miR-138 in different cancer types (16-18). Considering various functions and heterogenous targets in different types of cancers, miR-138 could be regarded as a propitious remedial strategy for cancer (19).

MiR-138 negatively regulated FOXC1 to suppress the malignant progression of PCa (20, 21). MiR-138 was also incorporated in the suppression of the Wnt/β-catenin pathway in PCa (22). Furthermore, miR-138 and *CCND1* expression exhibited a reverse correlation in nasopharyngeal carcinoma (NPC), but this association has not been examined in PCa and other cancer types (14). High *CCND1* expression was also correlated with progressive malignancy in PCa (23, 24). *CCND1* (located on chromosome 11q13) functions as an essential coordinator in cell cycle progression from G1 (growth) to the S phase (synthesis) (25). Overexpression of *CCND1* was discovered in several types of cancer as an oncogene. This oncogenic behavior might be through diverse mechanisms such as disturbing cell cycle, proliferation, and neoplastic cell transformation (26-30).

In the present research, we intended to discover the target genes for miR-138 and corroborate the importance of miR-138 in tumorigenesis in PCa. Bioinformatics analysis was carried out to explore the target genes of miR-138 and discover their expression pattern. We assigned seven target genes for miR-138: *ABL1*, *CCND1*, *CCND3*, *VIM*, *TWIST1*, *HIF1A*, and *TERT*. Among them, *CCND1* emerged as a possible contributor to miR-138-regulated tumorigenesis due to its higher expression in PCa. As such, we characterized the expression profile of miR-138 in PCa cell lines, a non-cancer cell line, PCa, and benign prostatic hyperplasia (BPH) clinical samples. Moreover, the expression profile of *CCND1* in PCa cell lines, a non-cancer cell line was evaluated. The inverse regulatory function of miR-138 on *CCND1* was examined by luciferase assay. We also investigated the impact of transient overexpression of miR-138 on the cell proliferation and expression of *CCND1* in PCa cell lines to exhibit whether miR-138 is capable of hindering the proliferation of PCa cells via moderating *CCND1*.

Materials and Methods

MiRNA prediction

MiR-138 complementary sequences located within the 3′-UTR of target mRNAs were regarded as target sequences. PicTar (http://pictar.mdc-berlin.de), TargetScan (www.targetscan.org), Mirtargetlink2 (https://ccb-compute.cs.uni-saarland.de/mirtargetlink2) and mirdb (http://www.mirdb.org/) were used for this purpose. These programs combine seed matches, conservation analysis, the thermodynamic stability of miRNA-mRNA duplexes, and site accessibility, among other characteristics, to maximize the target prediction specificity (31). Total scores computed by each tool were calculated, and genes with the maximum score were considered as target genes. The number of target sites, GC content of the seed site, and nearness of any base pairing to promote the accessibility of miRNA to the mRNA response element were examined manually in the computational programs to predict the best-presumed mRNAs. Based on previous reports, genes that were substantially upregulated in the other cancer types were also considered.

Samples

Thirty-five specimens of prostate cancer and 15 specimens of BPH were taken during radical prostatectomies. Clinical samples were provided by the Department of Pathology, Hashemi Nejad Hospital (Tehran, Iran) between 2014 and 2015. All volunteers were informed and filled out

the consent form. The research was approved by the ethical committee of the Pasteur Institute of Iran (#825 and #1010 and #7967). Gleason score, pathological stage, and histological prognosis were evaluated based on the guidelines of the Union for International Cancer Control (32). These samples were used in our previous work, where we described the patient demographics and clinicopathological features in detail (33).

Cell culture

PC3 and DU145 as human PCa cell lines were supplied by Leibniz-Institute DSMZ (Germany). DU145 cells were grown in RPMI 1640 medium reinforced with 10% FBS (Gibco, USA). PC3 cells were maintained in a 1:1 mixture of Ham's F12 and RPMI 1640 medium (10% FBS). HUVEC (Human umbilical vein endothelial cell line) was provided by the National Cell Bank of Iran and was maintained in a 1:1 mixture of Ham's F12 and DMEM medium (20% FBS). The cells were cultured in 5% CO2 and 37 °C.

RNA extraction and reverse transcription

RNA extraction of PC3, DU145, HUVEC cell lines, and clinical samples was conducted based on previously described protocols (33). The ratio of absorbance at 260 nm and 280 nm was considered as the purity index of the extracted RNA. After that, 1.5 µg of each extracted RNA was applied for cDNA synthesis by PrimeScript RT reagent kit based on the manufacturer's instruction (Takara Bio, Japan). Reverse transcription of miRNA was the same as mRNA except for designed stem-loop RT primers which substituted for oligo dT primers.

Quantitative reverse transcription polymerase chain reaction (RT-qPCR)

The expression of different mRNA was studied by a Rotor-Gene 6000 system (Corbett Life Science; Qiagen, Germany). Mixture for RT-qPCR with the ultimate volume of 20 µl included 10µl SYBR Green Master Mix (Takara, Japan), 0.5 pMol of the target specified primers (Table 1), and 1 µL of cDNA. The protocol of RT-qPCR included an initial denaturation at 95 ºC for 30 seconds, followed by 40 cycles of 95 ºC for 5 seconds and 60 ºC for 30 seconds. The mixture for Real-Time PCR with the total volume of 20 µl was comprised of 10 µl qPCR Master mix, 1 µl universal reverse-primer, 1 µl specific forward primer, and 1 µL cDNA. The thermocycling protocol consisted of an initial denaturation at 95 ˚C for 15 minutes, 40 cycles of 94 ˚C for 15 seconds, 55 ˚C for 30 seconds, and 70 ˚C for 30 seconds. The expression of mRNA was normalized with *GAPDH*. The *SNORD47* (U47) and U6 miRNAs were applied to normalize miRNA expression. The normalization of the target gene with the reference standard was performed using REST © (relative expression software tool). The relative expression was founded upon the expression ratio of the target genes in contrast with the reference gene. The ratio of mRNAs to miRNAs was calculated using the $\Delta\Delta C_T$ method. The average C_T values of the target gene were subtracted from the C_T of the housekeeping gene to calculate ΔC_T. The results were analyzed in GraphPad. The proliferation efficiency of RT-qPCR was evaluated using serial dilutions of 10^1, 10^2, and 10^3 of a pooled cDNA sample (15 samples) for every primer set, besides normalizing against references.

Table 1. Specific primers were designed for seven target genes predicted by computational tools.

AACGGGAAGCTTGTCATCAATGGAAA GCATCAGCAGAGGGGGCAGAG	GAPDH
GCTGTTATCTGGAAGAAGCCCT GCAACGAAAAGGTTGGGGTC	ABL1
GACCTTCGTTGCCCTCTGTG GAGGCGGTAGTAGGACAGGA	CCND1
CTCCCCAAAGGCAGGCTC GCAAGACAGGTAGCGATCCA	CCND3
GTACAAATCCAAGTTTGCTGACCTC TTAAGGGCATCCACTTCACAGG	VIM
CTCAGCTACGCCTTCTCCGT CGAATGCATCCCAATTCCACT	TWIST1
TCCAAGAAGCCCTAACGTGT ATGTTCCAATTCCTACTGCTTGA	HIF1A
GTGCTACGGCGACATGGAGA GGGCATAGCTGAGGAAGGTTT	TERT

Luciferase assay

The probably paired sequences of 3′-UTR of the *CCND1* gene were found from miRTarBase, which sums up the interaction sites reported in previous studies and predicts specific interactions (14). Three interactional regions in 3′-UTR of *CCND1* predicted by miRTarBase, including regions 757-776, 3096-3118, and 1457-1497 (NM_053056.3), were synthesized (Biomatik, Canada), and subcloned into the XhoI/NotI restriction sites of psiCHECK™-2 Vector (Promega, USA) consecutively with 20 nucleotides in between. The final construct was named psiCHECK2-*CCND1*-3′UTR. Syncel-miR-39-3p (negative control, abm, Canada) and miR-138-5p (miR-138 mimic) sequence vectors were purchased from Qiagen, Germany. Initially, about 10^3 PC3 cells were grown in a 96-well plate. After 12-16 hours, psiCHECK2-*CCND1*-3′, miR-138-5p-mimic+psiCHECK2-*CCND1*-3′UTR, and Syn-cel-miR-39-3p+psiCHECK2-*CCND1*-3′UTR were co-transfected into the PC3 cells in triplicates. Dual-Luciferase Reporter Assay System (Promega, USA) was adopted to evaluate the luciferase activity 24 hours after transfection, based on the manufacturer's instruction as previously elucidated (34). The multi-well plate luminom-

eter Renilla luciferase activity was normalized against firefly luciferase.

Cell proliferation analysis

The viability of transfected cells with miR-138 was examined using MTT (3-(4, 5-dimethylthiazol-2-Yl)-2, 5-diphenyltetrazolium bromide, Sigma, Germany) assay. Briefly, about 10^3 PC3 and DU145 cells were grown in every well of a 96-well plate and transfected with miR-138-5p-mimic and Syn-cel-miR-39-3p. The cells that had only been incubated with Lipofectamine were used as control. The optical density was read at 540 nm against 630 nm as the reference. Cell proliferation was interpreted respective to non-transfected cells.

Statistical analysis

Statistical analysis was conducted utilizing the mean ± standard error of mean (SEM) in the GraphPad Prism version 8.01 (GraphPad, USA). The difference among the various categories was calculated using Analysis of variance (ANOVA) followed by Tukey's multiple comparisons test. *P values* ≤ 0.05 were deemed as noteworthy. All assays were conducted at least in triplicate.

Results

Identification of miR-138 candidate target genes in PCa

As indicated in table 2, a total of seven genes were selected based on previously validated genes in papers, and the highest scores in Target Scan, Microcosm, PicTar, and miRanda: *ABL1* (ABL proto-oncogene 1, non-receptor tyrosine kinase), *CCND1* (cyclin D1), *CCND3* (cyclin D3), *VIM* (vimentin), *TWIST1* (twist family bHLH transcription factor 1), *HIF1A* (hypoxia-inducible factor 1 subunit alpha), and *TERT* (telomerase reverse transcriptase) genes.

MiR-138 overexpressed in PC3 and DU145 cells, but for HUVEC it declined

The expression of miR-138 was examined in PCa cell lines in comparison with HUVEC, as a normal cell line utilizing RT-qPCR. HUVEC was selected as a normal control in line with the earlier researches (33, 35). U6 or U47 genes functioned as normalizers. Mean ± SEM values are represented in Table 1s. As displayed in Figure 1, miR-138 obviously overexpressed in HUVEC cells in comparison with PC3 and DU145 using U6 or U47 as normalizer (*p*-value<0.0001). Interestingly, the expression of miR-138 exhibited no substantial variations between DU145 and PC3 cell lines using U6 and U47 as normalizers.

The expression of miR-138 diminished in the PCa specimens, as compared with BPH clinical samples

The expression of miR-138 in PCa and BPH clinical samples was examined via RT-qPCR. U6 and U47 genes functioned as normalizers. Mean ± SEM values of these comparisons are represented in Table 2s. The expression of miR-138 evidently diminished in PCa clinical samples in comparison with BPH tissues using U6 (*p*-value=0.0030) and U47 (*p*-value=0.0003) as normalizers (Figure 2).

Among seven candidate genes, only *CCND1* enhanced in PCa cell lines

To evaluate the influence of reduced amounts of miR-138 on PC3 and DU145 cancer cells, the expression profile of seven selected target genes, including *ABL1*, *CCND1*, *CCND3*, *VIM*, *TWIST1*, *HIF1A*, and *TERT* genes was examined utilizing RT-qPCR. PCR efficiency of every sample

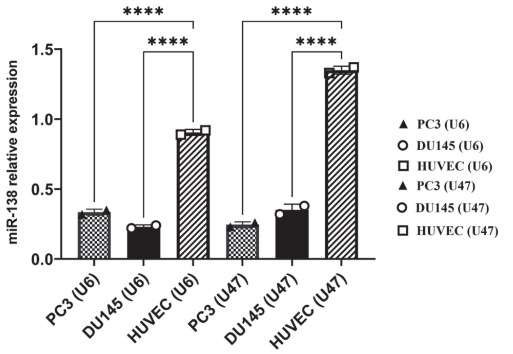

Figure 1. Results of quantitative RT-PCR on PCa and HUVEC cell lines: relative expression ($2^{-\Delta\Delta CT}$) of miR-138 in HUVEC cells compared to PC3 and DU145. U6 or U47 housekeeping genes were applied as the normalizers. **** is p-value equal or less than 0.00005.

Table 2. Selection of miR-138 target genes using four computational algorithms and considering previously validated genes in papers*.

Gene Symbol	miRDB	PicTar	Target scan	Mirtargetlink2	Validated genes in papers	Overall score
ABL1	0	0	1	0	1	2
CCND1	1	0	1	1	1	4
CCND3	1	0	1	1	1	4
VIM	1	0	1	1	1	4
TWIST1	0	0	1	1	1	3
HIF1A	1	1	1	1	1	5
TERT	0	0	0	1	1	2

* 1: MiR-138 targets a specific gene, 0: MiR-138 does not target a specific gene.

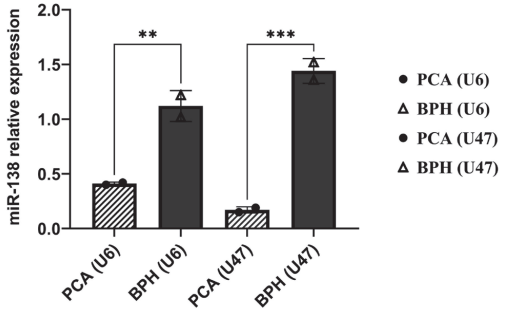

Figure 2. Results of quantitative RT-qPCR on PCa tissue samples and BPH samples: relative expression ($2^{-\Delta\Delta CT}$) of miR-138 in PCa tissue samples compared with BPH samples. U6 or U47 housekeeping genes were applied as the normalizers. ** is p-values equal or less than 0.005. *** is p-values equal or less than 0.0005.

was between 95% to 105%, based on the slope of the standard curve (Figure1s a, b). Moreover, the relative expression of *ABL1*, *CCND1*, *CCND3*, *VIM*, *TWIST1*, *HIF1A*, and *TERT* genes was compared to *GAPDH* as the control group (These target genes were previously normalized to *GAPDH* to quantify their relative expression). As elucidated in Figure 3 (a), among seven evaluated target genes, only *CCND1* was expressed at a significantly higher level (*p*-value=0.0016) in comparison with *GAPDH* as the housekeeping gene in PC3 cells. The expression of *CCND1* insignificantly raised in the DU145 cell line compared to the control group, as elucidated in Figure 3 (b). The expression of other candidate genes, including *ABL, CCND3, VIM, TWIST1, HIF1A*, and *TERT,* displayed no substantial change in comparison with *GAPDH* in PC3 and DU145 cell lines. Mean ± SEM values of the expression level of these genes are represented in Table 3s.

The expression of *CCND1* was reversely correlated with miR-138 in PCa cell lines

Pearson correlation test was performed between the expression miR-138 and *CCND1* gene in PC3 and DU145 cell lines, to explore whether the *CCND1* expression was coordinated with the level of miR-138. As displayed in figure 4 (a), the augmented level of *CCND1* was correlated to the declined miR-138 expression using U6 (R=−-0.9998, P=0.0135) and U47 (R=-0.9999, P=0.0074) as normalizers in the PC3 cell line. Moreover, *CCND1* exhibited a reverse correlation with miR-138 using U6 (R=-0.9982, P=0.0378) and U47 (R=-0.9995, P= 0.0203) as normalizers in DU145 cell line (figure 5, b). The results may propose the modulatory impact of miR-138 on the expression profile of *CCND1*.

CCND1 was corroborated as the target of miR-138 in the PC3 cell line by luciferase assay

MiRanda was utilized to analyze and predict 3′UTR sequences of the *CCND1* gene that could be targeted by miR-138. MiR-138-complementary sites located on the 3′ noncoding region of *CCND1* transcripts in miRTarBase are represented in Figure 5. To examine and corroborate the impact of miR-138 on *CCND1*, the predicted 3′UTR sequences of *CCND1* were cloned downstream of luciferase in the psiCHECKTM-2 vector. PC3 cells were transfected in three groups: psiCHECK2-*CCND1*-3′UTR plus miR-138-

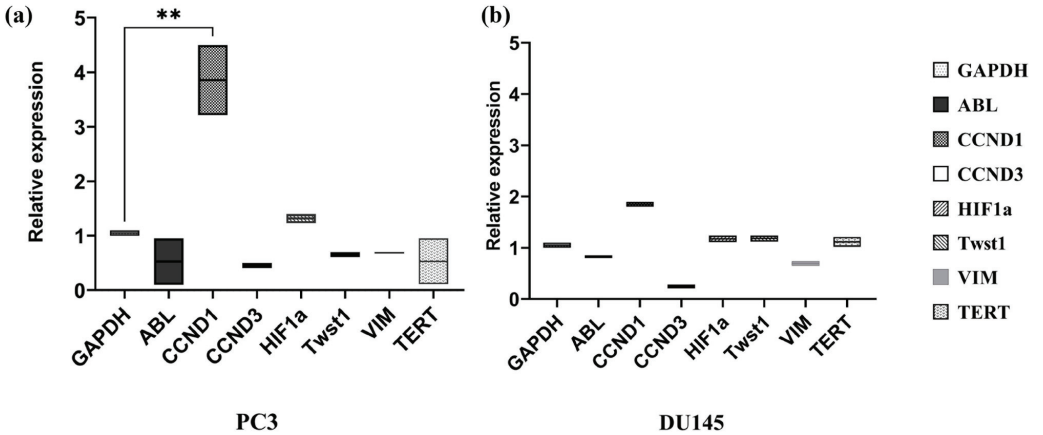

Figure 3. Results of quantitative RT-PCR on all candidate genes in PC3 and DU145 cell lines. (a) Substantial overexpression of *CCND1* in comparison with *GAPDH* as a housekeeping gene in PC3 cells. The expression profile of other candidate genes, including *ABL, CCND3, VIM, TWIST1, HIF1A, and TERT* genes exhibited no considerable change in comparison with *GAPDH* in the PC3 cell line. (b) An insignificant rise in the expression of *CCND1* in the DU145 cell line. The expression of other candidate genes, including *ABL, CCND3, VIM, TWIST1, HIF1A, and TERT* genes, revealed no substantial change in comparison with *GAPDH* in the DU145 cell line. ** is p-values equal or less than 0.005.

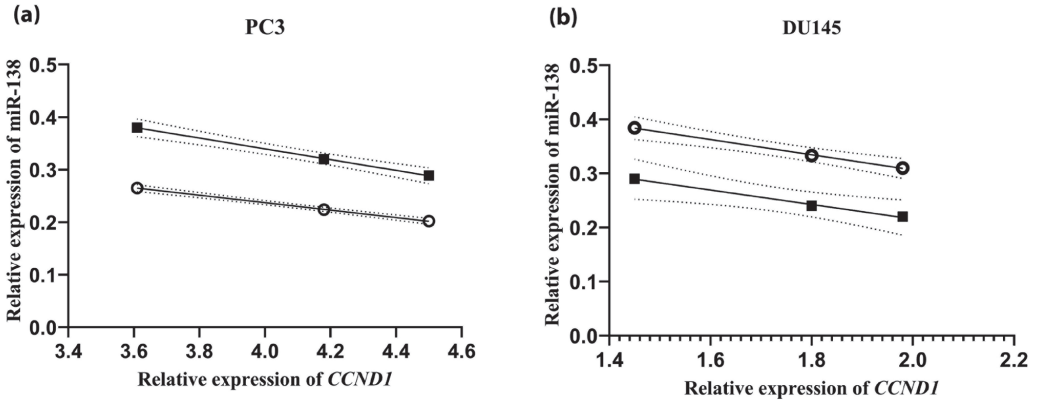

Figure 4. Pearson correlation analysis was applied to examine the correlation between the expression of miR-138 and the CCND1 gene in PCa cell lines. (a) A substantial negative correlation between the expression of CCND1 gene and miR-138 was noted using U6 (Y = -0.1026*X + 0.7500, R^2=0.9996) and U47 (Y = -0.07092*X + 0.5209, R^2= 0.9999) as normalizers in PC3 cell lines. (b) A substantial negative correlation between the expression of CCND1 gene and miR-138 was observed using U6 (Y = -0.1335*X + 0.4828, R^2=0.9965) and U47 (Y = -0.1405*X + 0.5872, R^2= 0.9990) as normalizers in DU145 cell lines.

-5p-mimic, psiCHECK2-*CCND1*-3′UTR plus Syn-cel-miR-39-3p, and psiCHECK2-*CCND1*-3′UTR alone. Mean ± SEM values of luciferase activity in transfected PC3 cells are represented in Table 4s. As elucidated in Figure 6, miR-138-5p-mimic diminished the efficacy of luciferase compared to psiCHECK2-*CCND1*-3′UTR plus Syn-cel-miR-39-3p (*p*-value = 0.0016), and psiCHECK2-*CCND1*-3′UTR alone (*p*-value = 0.0022). While no substantial variation was noted between the psiCHECK2-*CCND1*-3′UTR plus Syn-cel-miR-39-3p transfected cells, and the psiCHECK2-*CCND1*-3′UTR transfected cells. The data of the luciferase assay evidenced that transfection of miR-138-5p-mimic considerably diminished Renilla luciferase activity, and it turned out that miR-138 could modulate the *CCND1* expression through acting on its 3′-UTR in the PC3 cell line.

MiR-138-5p-mimic diminished the expression of *CCND1* in the transient transfected PCa cell lines

RT-qPCR was utilized to evaluate the expression of *CCND1* in the miR-138-5p-mimic transfected PC3 and DU145 cells to realize whether miR-138 could modulate *CCND1* by acting on its 3′-UTR in PCa cell lines. As dis-

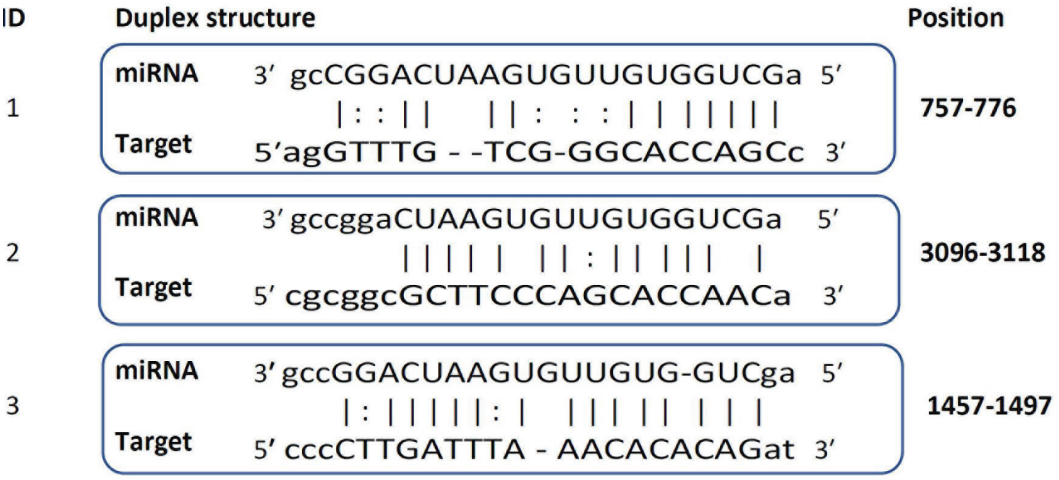

Figure 5. The complementary sequence of miR-138 located in the 3′-UTR of *CCND1* transcripts. Three interactional regions in 3′-UTR of *CCND1* were predicted by miRTarBase, including regions 757-776, 3096-3118, and 1457-1497 (NM_053056.3).

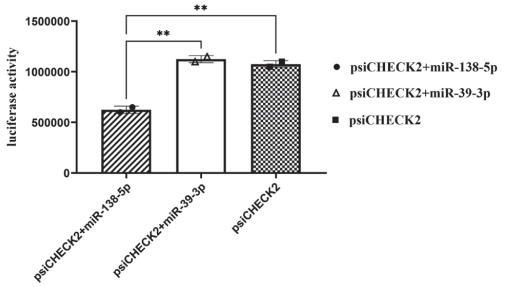

Figure 6. Impact of miR-138 on the expression of *CCND1*: PC3 cells were transfected with Renilla luciferase expression cassette, psiCHECK2 carrying the 3′-UTR of *CCND1* alone, psiCHECK2-*CCND1*-3′UTR+miR-138-5p-mimic, and psiCHECK2-*CCND1*-3′UTR+Syn-cel-miR-39-3p. MiR-138-5p-mimic transfected PC3 cells notably exhibited diminished Renilla luciferase activity. ** is p-values equal or less than 0.005.

played in Figure 7, the expression of CCND1 insignificantly diminished following transfection with miR-138-5p-mimic in DU145 cells, while *CCND1* mRNA level significantly decreased following transfection in PC3 cells (*p*-value = 0.0008). Mean ± SEM values of the expression level of CCND1 in transfected PC3 and DU145 cells compared with non-transfected cells are represented in Table 5s.

In conclusion, *CCND1* expression revealed a tendency to decrease in DU145 cell lines and a substantial decline in PC3 cells. Diminished expression of *CCND1* in miR-138 transfected PC3 and DU145 cell lines implies the suppressive influence of miR-138 on the expression of *CCND1* in the PCa cell lines.

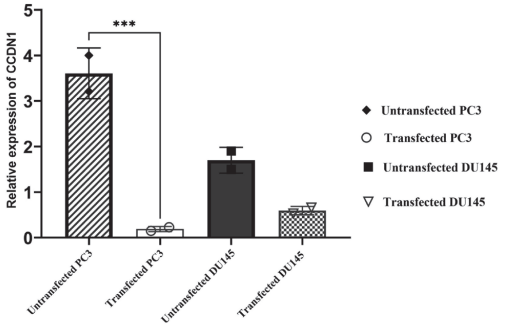

Figure 7. The impact of miR-138-5p-mimic transient transfection on the expression of *CCND1*: The expression of *CCND1* in miR-138-5p-mimic transfected PC3 and DU145 cells was examined by RT-qPCR. The expression of CCND1 in miR-138-5p-mimic transfected DU145 cells insignificantly lessened, while CCND1 mRNA level substantially reduced following transfection in PC3 cells. The results were normalized to the *GAPDH* housekeeping gene. *** is p-values equal or less than 0.0005.

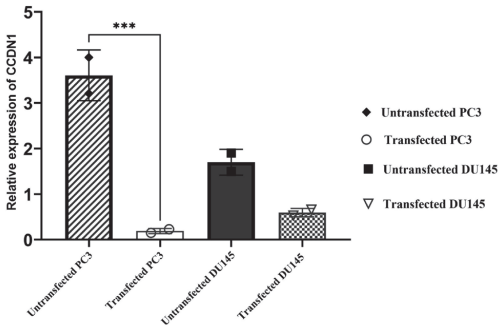

Figure 8. MTT test was utilized to examine the proliferation rate of PC3 and DU145 cells transfected in three groups, including miR-138-5p-mimic, Syn-cel-miR-39-3p, and Lipofectamine alone. MiR-138-5p-mimic transfected cell lines showed reduced proliferation in comparison with non-transfected cell lines. * is p-values equal or less than 0.05. ** is p-values equal or less than 0.005. *** is p-values equal or less than 0.0005.

MiR-138-5p-mimic could have a pivotal function in the inhibition of cell proliferation in the transient transfected PCa cell lines

The cell viability test by MTT was carried out to understand the functional activity of overexpression of miR-138 in the proliferation of PCa cell lines. Cells receiving only Lipofectamine (blank) were utilized as the negative control, and cells with no transfection functioned as the external control group. PC3 and DU145 cells were transfected in three categories containing miR-138-5p-mimic and Syn-cel-miR-39-3p in addition to the cells incubated only with Lipofectamine. Mean ± SEM values of the proliferation scale in PC3 and DU145 cells transfected in three groups are represented in Table 6s. The outcome of the MTT assay implied that the proliferation of PC3 cells 24 hours subsequent to transfection with miR-138-5p-mimic significantly declined compared to Syn-cel-miR-39-3p transfected cells (*p*-value =0.0006) and Lipofectamine incubated cells (*p*-value =0.0011). Furthermore, miR-138-5p-mimic transfected DU145 cells substantially evidenced a diminished proliferation rate compared with Lipofectamine incubated cells (*p*-value=0.0122), while miR-138-5p-mimic and Syn-cel-miR-39-3p transfected cells expressed insubstantial variations (Figure 8).

In conclusion, the proliferation of all miR-138-5p-mimic transfected cell lines considerably diminished compared to non-transfected cell lines.

Discussion

During the first phases of cancer diagnosis, miRNAs are being used more and more. They are also utilized for the therapy and prognosis of this disease (13). Disorganization of miRNAs is wholly proven to implicate the advance and furtherance of cancer cells (36-38). As elucidated before, expression of the microRNAs inclusive of miR-26a, miR-138, miR-1266, miR-185, and miR-30c diminished in PCa tissues and cell lines (27, 32). Moreover, miRNA expression profiles showed widespread dysregulation in primary PCa compared to normal prostate tissue.(36) As expounded earlier, miR-138 arrested the malignant advancement of several human cancers, including pancreatic cancer, colorectal cancer, and other cancer types (10, 12, 39, 40). Here, distinctive expression of miR-138 was scrutinized in PCa tissues and cell lines in comparison with non-cancerous cell lines and BPH tissues, respectively. We corroborated that the expression of miR-138 considerably lessened in PCa cell lines in comparison with the HUVEC cell line. Additionally, miR-138 obviously diminished in PCa tissues in comparison with BPH clinical samples. These findings were in line with previous studies where miR-138 evidently lessened in PCa tissues and cell lines (19, 20, 22).

Here, according to bioinformatic analysis with online software such as Target Scan, Microcosm, PicTar, and miRanda, it was assumed that *ABL1, CCND1, CCND3*, *VIM*, *TWIST1, HIF1A,* and *TERT* might be the target gene of miR-138. In accordance with RT-qPCR findings, the expression of *CCDN1* substantially augmented in PCa tissue and PC3 cell line and had an insignificant rise in the DU145 cell line. Furthermore, the correlation between the expression of *CCND1* and miR-138 was calculated in PC3, DU145 cell lines. Our data proposed that *CCND1* showed a reverse correlation with the miR-138 in the prostate cancer cell lines.

Additionally, dual-luciferase reporter assay was utilized to explore the associations between miR-138 and 3' UTR of *CCND1* and to examine whether this relationship is influential in the PCa progress. In accordance with the results of the luciferase reporter assay, overexpression of miR-138 prohibited the expression of *CCDN1* in PC3 cell lines. It was inferred that miR-138 could negatively regulate the expression of *CCDN1* in PCa cell lines. As pointed out previously, a reverse correlation was distinguished between miR-138 and the expression of *CCND1* in nasopharyngeal carcinoma (14). *CCND1* has also been associated with miRNAs in other tumorigenesis pathways in PCa. In a new signaling pathway comprising *LOXL1-AS1*, miR-541-3p, and *CCND1,* which modulates the cell cycle and proliferation of PCa cells, *CCND1* expounded as the target of miR-541 (41). Additionally, owing to the post-transcriptional regulatory function of the miR17 family, *CCND1* evidently elevated when the miR17 family was suppressed in PCa cell lines (42).

Subsequently, we scrutinized the influence of miR-138 overexpression on the expression profile of *CCDN1* in the transiently transfected PC3 and DU145 cell lines. Conclusively, overexpression of miR-138 could repress *CCDN1* expression in PC3 cells, while the expression level of the *CCDN1* gene exhibited an insignificant reduction in the DU145 cell line. MiR-138 has also shown other negative regulatory influences on PCa. As previously elucidated, overexpression of miR-138 substantially arrested the capability of the Wnt/β-catenin pathway in C4-2B and PC3 cells. Accordingly, miR-138 reversely modulates β-catenin in prostate cancer cells (22).

MTT assay was utilized to appraise the inhibitory function of miR-138 on the proliferation scale of PCa cell lines. Our findings revealed that miRNA-138 could precipitate an anti-proliferative effect on PCa cells, which was in line with preceding research that miR-138 motivated anti-proliferative influence on several cancers such as clear cell renal cell carcinoma, squamous cell carcinoma, tongue squamous cell carcinoma, and head and neck squamous cell carcinomas (38-40). Consonant with the earlier investigation, miR-138 and its target CCND1 were implicated in the modulation of the nasopharyngeal carcinoma progress. Overexpression of miR-138 also induced arrest in the G_1 cell cycle, repression of cell proliferation *in vitro,* and inhibitory effects on the tumorigenicity of mice xenografts (14). Moreover, it was previously declared that overexpression of miR-138 hindered the metastasis and proliferation of PCa through targeting and downregulating FOXC1 (20). Furthermore, earlier experiments revealed that elevated expression of miR-17 family members contributed to the lessening of *CCND1* which resulted in motivated apoptosis, suppressed proliferation capability, and colony forming potential (42). MiR-138 and PD-L1 also exhibited a negative correlation in colorectal cancer. The diminished proliferation rate in miR-138-5p mimic transfected HCT116 and SW620 cells was evidenced by MTT assay through regulating PD-L1 as the target gene (39). In the current research, the potential of miR-138 to suppress cell proliferation indicated its function as a tumor suppressor in PCa, which might be partial via regulating *CCND1* as the target gene. Our results were in line with previous research that miR-138 repressed proliferation and motivated apoptosis through modulating multiple targets (43, 44). MiR-138 also functioned in the modulation of enhancer of zeste homolog 2 (EZH2) to repress proliferation efficiency, motivate apoptosis and arrest G0/G1 cell cycle as a tumor suppressor in non-small cell lung cancer cells (45).

Therefore, miR-138 elucidated assorted biological functions through modulating the *CCDN1* gene in PCa. *CCND1* showed an inverse correlation with the miR-138 level in PCa cell lines. It implies the reverse modulatory impact of miR-138 on the expression of *CCDN1* in PCa. However, the antiproliferative effects of miR-138 could be applied through the mechanisms other than *CCDN1* regulation in the DU145 cell line. Further studies are required to identify the cooperative genes. Distinguishing these functional targets might have clinical importance hereafter. Our findings need more complementary studies, such as evaluating the repressive influence of miR-138 on the malignant advancement of PCa in vivo as well as clinicopathological features of PCa patients through analysis of the biological function of CCND1.

Here, to the best of our knowledge, we evidenced the direct association of miR-138 with the *CCND1* gene for the first time in PCa. The overexpression of *CCND1* was also negatively correlated with miR-138 in PCa cell lines. Our findings implied that miR-138 could modulate the enhanced expression of *CCND1* to some extent. Conclusively, miR-138 functions as a tumor suppressor through the moderation of the *CCND1* gene in the malignant advancement of PCa.

Conclusions

Our findings revealed an etiological relationship between miR-138 and *CCND1* gene as its target in PCa. We also corroborated the functionality of this correlation in the growth and proliferation of PCa that could function in miRNA-based diagnostic and therapeutic approaches. However, further comprehensive evaluation of the modulatory pathways and molecular mechanisms in PCa would highly facilitate the promotion of design and selection of targets for therapeutic procedures.

Declaration statements

Ethics approval and consent to participate: The study was carried out in accordance with the guidelines of the Ethics Committee of Pasteur Institute of Iran (#825, #1010, and #7967). Informed consent was obtained from all subjects involved in the study.

Consent for publication: Not Applicable.

Availability of data and material: The supporting data of the findings of this study are available by the corresponding author upon reasonable request.

Competing interest: The authors declare that they have no competing interests.

Funding: This study was granted by the Pasteur Institute of Iran.

Authors' contributions: Project administration, conceptualization, supervision, writing, review, and editing: Pezhman Fard-Esfahani. Preparation of the manuscript, interpretation, and analysis of data: Nasrin Haghighi-Najafabadi. Revision of the manuscript: Ghazal Haddad. Methodology: Shima Fayaz, Mahboubeh Berizi.

Acknowledgment: We thank the staff of the Biochemistry Department (Pasteur Institute of Iran). This study was funded as research project by Pasteur Institute of Iran.

References

1. Sung H, Ferlay J, Siegel RL, Laversanne M, Soerjomataram I, Jemal A, et al. Global cancer statistics 2020: GLOBOCAN estimates of incidence and mortality worldwide for 36 cancers in 185 countries. CA: a cancer journal for clinicians. 2021;71(3):209-49.
2. Etzioni R, Penson DF, Legler JM, Di Tommaso D, Boer R, Gann PH, et al. Overdiagnosis due to prostate-specific antigen screening: lessons from US prostate cancer incidence trends. Journal of the National Cancer Institute. 2002;94(13):981-90.
3. Duffy MJ. Biomarkers for prostate cancer: prostate-specific antigen and beyond. Clinical Chemistry and Laboratory Medicine (CCLM). 2020;58(3):326-39.
4. Filella X, Foj L. Novel biomarkers for prostate cancer detection and prognosis. Cell & Molecular Biology of Prostate Cancer. 2018:15-39.
5. Bartel DP. MicroRNAs: target recognition and regulatory functions. cell. 2009;136(2):215-33.
6. Lu J, Getz G. Mis ka EA, Al va rez-Sa a ved ra E, Lamb J, Peck D, et al. Mic roR NA ex pres si on pro fi les clas sify hu man can cers Na tu re. 2005;435(7043):834-8.
7. Rivera-Barahona A, Pérez B, Richard E, Desviat LR. Role of miRNAs in human disease and inborn errors of metabolism. Journal of inherited metabolic disease. 2017;40(4):471-80.
8. Tutar Y. Editorial (Thematic issue:"miRNA and cancer; computational and experimental approaches"). Current pharmaceutical biotechnology. 2014;15(5):429-.
9. Filipów S, Łaczmański Ł. Blood circulating miRNAs as cancer biomarkers for diagnosis and surgical treatment response. Frontiers in genetics. 2019;10:169.
10. Zhu Z, Tang J, Wang J, Duan G, Zhou L, Zhou X. MiR-138 acts as a tumor suppressor by targeting EZH2 and enhances cisplatin-induced apoptosis in osteosarcoma cells. PloS one. 2016;11(3):e0150026.
11. Jiang B, Mu W, Wang J, Lu J, Jiang S, Li L, et al. MicroRNA-138 functions as a tumor suppressor in osteosarcoma by targeting differentiated embryonic chondrocyte gene 2. Journal of Experimental & Clinical Cancer Research. 2016;35(1):1-9.

12. Xiao L, Zhou H, Li X-P, Chen J, Fang C, Mao C-X, et al. MicroRNA-138 acts as a tumor suppressor in non small cell lung cancer via targeting YAP1. Oncotarget. 2016;7(26):40038.
13. Luu HN, Lin H-Y, Sørensen KD, Ogunwobi OO, Kumar N, Chornokur G, et al. miRNAs associated with prostate cancer risk and progression. BMC urology. 2017;17(1):1-18.
14. Liu X, Lv X-B, Wang X-P, Sang Y, Xu S, Hu K, et al. MiR-138 suppressed nasopharyngeal carcinoma growth and tumorigenesis by targeting the CCND1 oncogene. Cell cycle. 2012;11(13):2495-506.
15. Armand-Labit V, Pradines A. Circulating cell-free microRNAs as clinical cancer biomarkers. Biomolecular concepts. 2017;8(2):61-81.
16. Li J, Wang Q, Wen R, Liang J, Zhong X, Yang W, et al. MiR-138 inhibits cell proliferation and reverses epithelial-mesenchymal transition in non-small cell lung cancer cells by targeting GIT 1 and SEMA 4C. Journal of cellular and molecular medicine. 2015;19(12):2793-805.
17. Wang Y, Huang J-W, Li M, Cavenee WK, Mitchell PS, Zhou X, et al. MicroRNA-138 modulates DNA damage response by repressing histone H2AX expression. Molecular Cancer Research. 2011;9(8):1100-11.
18. Ye Xw, Yu H, Jin Yk, Jing Xt, Xu M, Wan Zf, et al. miR-138 inhibits proliferation by targeting 3-phosphoinositide-dependent protein kinase-1 in non-small cell lung cancer cells. The clinical respiratory journal. 2015;9(1):27-33.
19. Wang Y, Zhang Q, Guo B, Feng J, Zhao D. miR-1231 is downregulated in prostate cancer with prognostic and functional implications. Oncology Research and Treatment. 2020;43(3):78-86.
20. Zhang D, Liu X, Zhang Q, Chen X. miR-138-5p inhibits the malignant progression of prostate cancer by targeting FOXC1. Cancer Cell International. 2020;20(1):1-11.
21. Huang H, Xiong Y, Wu Z, He Y, Gao X, Zhou Z, et al. MIR-138-5P inhibits the progression of prostate cancer by targeting FOXC1. Molecular Genetics & Genomic Medicine. 2020;8(4):e1193.
22. Yu Z, Wang Z, Li F, Yang J, Tang L. miR-138 modulates prostate cancer cell invasion and migration via Wnt/β-catenin pathway. Molecular medicine reports. 2018;17(2):3140-5.
23. Fleischmann A, Rocha C, Saxer-Sekulic N, Zlobec I, Sauter G, Thalmann GN. High-level cytoplasmic cyclin D1 expression in lymph node metastases from prostate cancer independently predicts early biochemical failure and death in surgically treated patients. Histopathology. 2011;58(5):781-9.
24. Drobnjak M, Osman I, Scher HI, Fazzari M, Cordon-Cardo C. Overexpression of cyclin D1 is associated with metastatic prostate cancer to bone. Clinical Cancer Research. 2000;6(5):1891-5.
25. Xiong Y, Connolly T, Futcher B, Beach D. Human D-type cyclin. Cell. 1991;65(4):691-9.
26. Donnellan R, Chetty R. Cyclin D1 and human neoplasia. Molecular Pathology. 1998;51(1):1.
27. Ortiz AB, Garcia D, Vicente Y, Palka M, Bellas C, Martin P. Prognostic significance of cyclin D1 protein expression and gene amplification in invasive breast carcinoma. PloS one. 2017;12(11):e0188068.
28. Hedberg Y, Davoodi E, Roos G, Ljungberg B, Landberg G. Cyclin-D1 expression in human renal-cell carcinoma. International journal of cancer. 1999;84(3):268-72.
29. Comstock C, Revelo M, Buncher C, Knudsen K. Impact of differential cyclin D1 expression and localisation in prostate cancer. British journal of cancer. 2007;96(6):970-9.
30. Alao JP. The regulation of cyclin D1 degradation: roles in cancer development and the potential for therapeutic invention. Molecular cancer. 2007;6(1):1-16.
31. Peterson SM, Thompson JA, Ufkin ML, Sathyanarayana P, Liaw L, Congdon CB. Common features of microRNA target prediction tools. Frontiers in genetics. 2014;5:23.
32. Organization WH. National cancer control programmes: policies and managerial guidelines: World Health Organization; 2002.
33. Ostadrahimi S, Fayaz S, Parvizhamidi M, Abedi-Valugerdi M, Hassan M, Kadivar M, et al. Downregulation of miR-1266-5P, miR-185-5P and miR-30c-2 in prostatic cancer tissue and cell lines. Oncology letters. 2018;15(5):8157-64.
34. Ostadrahimi S, Valugerdi MA, Hassan M, Haddad G, Fayaz S, Parvizhamidi M, et al. miR-1266-5p and miR-185-5p promote cell apoptosis in human prostate cancer cell lines. Asian Pacific journal of cancer prevention: APJCP. 2018;19(8):2305.
35. Afgar A, Fard-Esfahani P, Mehrtash A, Azadmanesh K, Khodarahmi F, Ghadir M, et al. MiR-339 and especially miR-766 reactivate the expression of tumor suppressor genes in colorectal cancer cell lines through DNA methyltransferase 3B gene inhibition. Cancer biology & therapy. 2016;17(11):1126-38.
36. Wang R, Sun Y, Yu W, Yan Y, Qiao M, Jiang R, et al. Downregulation of miRNA-214 in cancer-associated fibroblasts contributes to migration and invasion of gastric cancer cells through targeting FGF9 and inducing

EMT. Journal of Experimental & Clinical Cancer Research. 2019;38(1):1-15.

37. Ding L, Zhang S, Xu M, Zhang R, Sui P, Yang Q. MicroRNA-27a contributes to the malignant behavior of gastric cancer cells by directly targeting PH domain and leucine-rich repeat protein phosphatase 2. Journal of Experimental & Clinical Cancer Research. 2017;36(1):1-13.
38. Li Q, Li Z, Wei S, Wang W, Chen Z, Zhang L, et al. Overexpression of miR-584-5p inhibits proliferation and induces apoptosis by targeting WW domain-containing E3 ubiquitin protein ligase 1 in gastric cancer. Journal of experimental & clinical cancer research. 2017;36(1):1-17.
39. Zhao L, Yu H, Yi S, Peng X, Su P, Xiao Z, et al. The tumor suppressor miR-138-5p targets PD-L1 in colorectal cancer. Oncotarget. 2016;7(29):45370.
40. Tian S, Guo X, Yu C, Sun C, Jiang J. miR-138-5p suppresses autophagy in pancreatic cancer by targeting SIRT1. Oncotarget. 2017;8(7):11071.
41. Long B, Li N, Xu X-X, Li X-X, Xu X-J, Liu J-Y, et al. Long noncoding RNA LOXL1-AS1 regulates prostate cancer cell proliferation and cell cycle progression through miR-541-3p and CCND1. Biochemical and biophysical research communications. 2018;505(2):561-8.
42. Dankert JT, Wiesehöfer M, Czyrnik ED, Singer BB, von Ostau N, Wennemuth G. The deregulation of miR-17/CCND1 axis during neuroendocrine transdifferentiation of LNCaP prostate cancer cells. PLoS One. 2018;13(7):e0200472.
43. Gao Y, Fan X, Li W, Ping W, Deng Y, Fu X. miR-138--5p reverses gefitinib resistance in non-small cell lung cancer cells via negatively regulating G protein-coupled receptor 124. Biochemical and biophysical research communications. 2014;446(1):179-86.
44. Huang B, Li H, Huang L, Luo C, Zhang Y. Clinical significance of microRNA 138 and cyclin D3 in hepatocellular carcinoma. journal of surgical research. 2015;193(2):718-23.
45. Zhang H, Zhang H, Zhao M, Lv Z, Zhang X, Qin X, et al. MiR-138 inhibits tumor growth through repression of EZH2 in non-small cell lung cancer. Cellular Physiology and Biochemistry. 2013;31(1):56-65.